

# Heat partitioning model with bubble tracking method considering bubble merger and stochastic nucleation site distribution

Hee Pyo Hong, Moonhee Choi, Hyoung Kyu Cho\*

Department of Nuclear Engineering, Seoul National Univ., 1 Gwanak-ro, Gwanak-gu, Seoul 08826

\*Corresponding author: chohk@snu.ac.kr

## 1. Introduction

In the nuclear industry, many attempts have been made to predict boiling heat transfer accurately. However, it has been challenging to predict boiling heat transfer with analytical and arithmetic models because many phenomena work in complex combinations. The most widely accepted arithmetic model for boiling heat transfer is the RPI model, proposed by Kurul and Podowski (1990) [1]. In the model, the heat flux is calculated by dividing it into evaporation, convection, and transient conduction based on the heat partitioning model. However, the model showed limitations in inclined and flow boiling conditions, and there have been improvements to overcome the limitations [2] [3]. Nevertheless, some important phenomena, such as a merger of bubbles, non-uniform nucleation site distribution, etc. could not be reflected realistically. For example, Gilman et al. [4] presented the modified-Hibiki model to consider interactions between multiple bubbles. This model assumed the suppression of bubble generation by applying a stochastic distribution to nucleation sites. Even with these improvements, the arithmetic prediction of boiling heat transfer has required significant simplifications. In this regard, Kim and Cho [5] proposed a new approach to effective predicting of boiling heat flux by simulating individual bubbles and their sliding.

In this paper, the heat partitioning model proposed by Kim and Cho [5] is revisited and applied for a horizontal upward heating plate geometry. At first, it is confirmed that the model can reproduce the same results of the RPI model if the same simplifications are applied. Then, the simplifications are removed one after another to quantify the effect of each assumption. Finally, the most dominant factor to the arithmetic prediction of boiling heat transfer and a future validation plan will be discussed.

## 2. Bubble tracking simulation

### 2.1 Simulation algorithm

The present numerical heat partitioning model simulates individual bubble using the evaporation heat transfer and force balance.

In the horizontal pool boiling condition, however, the bubble sliding does not occur so that individual bubble behavior can be tracked using the bubble growth simulation. To track all bubbles simultaneously, the calculations were performed in the sequence shown in Figure 1. Firstly, the domain to simulate is defined. Since

the number of nucleation sites changes depending on the wall temperature, the nucleation site density is calculated for a given wall temperature condition. The number of nucleation sites in the computational domain is initially determined for each calculation condition. It is assumed that the bubbles are generated repeatedly at the predetermined nucleation sites. Secondly, the generated bubbles are controlled according to the life cycle of the bubbles, such as growth, departure, merge, waiting, and nucleation. In the bubble growth part, the size of the bubble is determined based on the size in the previous time step and the growth model. Then, the size of the bubbles are compared with the calculated departure diameter in the bubble departure part. When its size exceeds the departure diameter, the bubble departs from the surface immediately. Thirdly, the distance between each bubble is calculated in the bubble merger part to determine the contact among bubbles. In this simulation, it was assumed that individual bubbles merge immediately upon contact to form a single spherical shape bubble, if they make contact. Finally, in the process of simulating waiting of the nucleation site, the location and size of the bubble calculated through the bubble merger are used to determine whether the site is occupied by a bubble or not. When it is not covered by a bubble, the time is counted as the waiting time. The accumulated time reaches the bubble waiting time, and then the nucleation starts again, and the same processes (growth, departure, merger, waiting) are repeated.

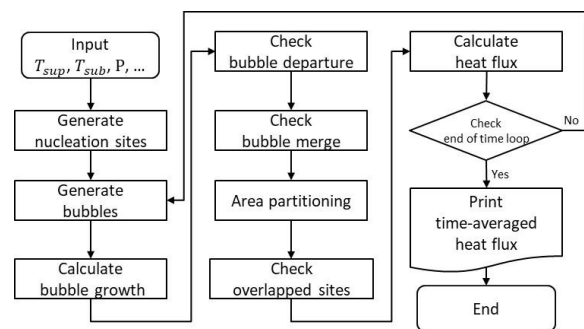


Fig. 1. Flow chart

### 2.2 Calculating heat flux with area partitioning

This section explains how to simulate area partitioning at each time step and calculate heat flux. The domain area is divided into bubble contact area, transient conduction area, and free convection area, as shown in Figure 2. In this study, the ratio of the diameter of the bubble contact area compared to the bubble diameter was assumed to be

constant. The heat flux in the bubble contact area was considered as evaporation heat flux and calculated by the volume of the bubble using Eq.(1)

$$q_{ev} = V_{total} \lambda \frac{\rho_v}{s}, \quad (1)$$

where to calculate evaporation heat flux, total departure volume ( $V_{total}$ ), vapor density( $\rho_v$ ), latent heat( $\lambda$ ), total simulation time(s) are used. The transient conduction occurs in the area where the bubble previously existed and but not occupied by the bubble contact area. The transient conduction heat flux can be calculated with Eq. (2)

$$q_{tc} = A_{tc} \frac{k_l}{\sqrt{t\pi\alpha_l}} (T_w - T_b), \quad (2)$$

where  $k_l$  and  $\alpha_l$  are thermal conductivity and thermal diffusivity of liquid, respectively.  $T_w$  and  $T_b$  are the wall and bulk temperature. Lastly,  $t$  is the time after the bubble departure. The transient conduction heat flux is calculated at every time step. The free convection area is defined as an area that does not correspond to the two areas above. The free convection heat flux can be calculated with Eq. (3).

$$q_{fc} = A_{fc} h_{fc} (T_w - T_b) \quad (3)$$

where  $h_{fc}$  is the convective heat transfer coefficient. At every time step, the heat flux corresponding to free convection and transient conduction are calculated based on each calculated region. Then, the total heat flux is calculated, as shown in Eq. (4), by adding the time-averaged value of the free convection and transient conduction heat flux and the heat flux due to evaporation at the end of the simulation.

$$q_{total} = q_{ev} + q_{fc} + q_{tc} \quad (4)$$

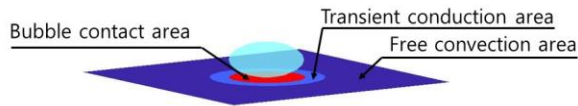


Fig. 2. Partitioned area

### 2.3 Simulation condition

Table. 1. Simulation condition

Pressure	1.013 bar
$T_{sup}$	0 ~ 30 K
$T_{sub}$	0 °C
$D_{bubble}/D_{contact}$	1
Influence area	1
Departure diameter	Tolubinsky's model[6]
Frequency	Cole's model[7]
Nucleation site density	Hibiki-Ishii model[8]

The conditions used in the simulation can be found in Table 1. All other conditions were fixed during the

simulation, and the wall temperature was changed from 0 to 30K with the pressure of 1 bar. For the baseline case, the bubbles were assumed to occur simultaneously and linearly grow during the growth time. The diameter of the bubble and the diameter of the bubble contact area were assumed to be the same, and the influence area was assumed to be 1.0. The remaining correlations needed to perform the simulation are listed in Table 1. After reproducing the RPI model using the baseline assumptions, realistic conditions were applied, which include the bubble contact area according to bubble growth, non-uniform nucleation site distribution, and stochastic nucleation timing.

### 3. Simulation results

Figure 3 shows examples of the simulations performed with three wall superheats. The number of nucleation sites increased with the wall temperature. The colors show the area of each heat transfer mechanism. Blue means the free convection and red means the bubble area. The other means transient condition, yellow indicates the strongest quenching, and the color of area approaches blue while quenching heat flux gets weaker.

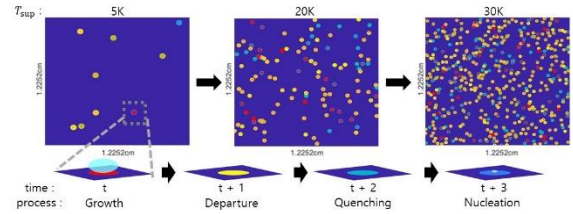


Fig. 3. Nucleation site distribution with wall superheats and life of single bubble

#### 3.1 Reproduction of the RPI model

For the baseline case, the analysis was performed with the same assumptions with the RPI model to verify the simulation in this study. The simulation result is shown in Figure 4. In order to reproduce the RPI model, the bubble contact area was fixed to the area corresponding to the departure diameter of the bubble. Also, because the RPI model does not consider the merge of the bubble, a uniform distribution was applied to prevent the merge effect of the bubbles. The result under these conditions showed that the total heat flux had an error of about 1% and matched well with the result of the RPI model.

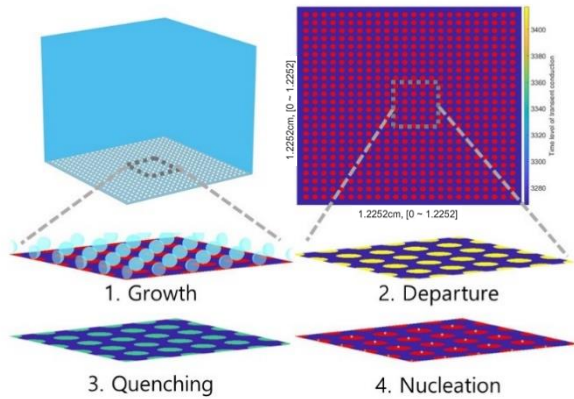


Fig. 4. Simulation results with reproduction of the RPI model

### 3.2 Changing bubble contact area according to bubble growth

In this case, the diameter of bubble contact area was changing linearly over time with bubble growth as shown in Figure 5 and Figure 6 shows the result of the change. As the bubble contact area decreased, the transient conduction area increased, resulting in a transient conduction heat flux increase by approximately 7% over the RPI model at 30K.



Fig. 5. Simulation modification with changing bubble contact area according to bubble growth

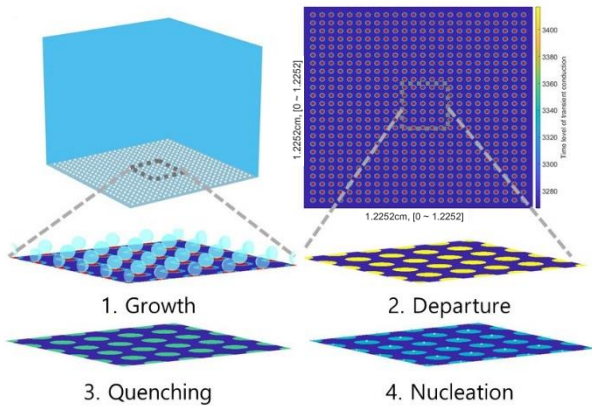


Fig. 6. Simulation results with changing bubble contact area according to bubble growth

### 3.3 Stochastic nucleation sites and bubble merger

In the previous section, the nucleation site was assumed to be uniform. To confirm the effect of the distribution, stochastic site conditions were applied. The results of the simulation are shown in Figure 7. The stochastic nucleation causes stochastic effects on the distance between bubbles. In that case, while simulation, the bubbles contact each other and start to merge. The merger allows the bubble's size to reach the departure diameter quickly, causing early departure. This early

departure causes the total bubble volume to reduce, which reduces the evaporation heat flux. In addition, since the area occupied by the bubble was decreased, it also reduces the transient conduction heat flux. Thus, the stochastic nucleation site causes a decrease in overall heat flux. With this effect, the heat flux at 30K, which has the most significant effect, is reduced by about 30% in evaporation and 22% in transient conduction compared to the model in which only the bubble contact area changes. Effects of the bubble merger on the total heat flux are shown in Figure 8.

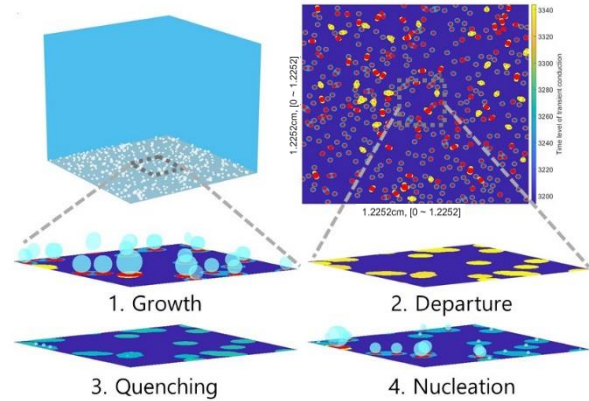


Fig. 7. Simulation results with stochastic nucleation sites and bubble merger

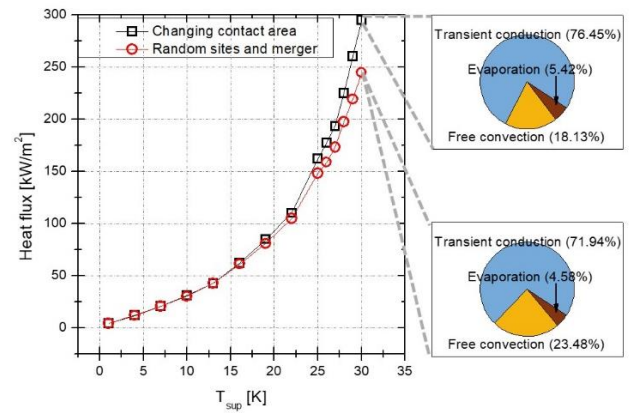


Fig. 8. Comparison of total heat flux with changing bubble contact area and including stochastic sites & merger

### 3.4 Stochastic nucleation timing

Lastly, the model was modified to allow bubbles to be nucleated with time discrepancies rather than simultaneous generation. The result of the modification is shown in Figure 9. Nucleation with the time discrepancies reduces the number of bubbles present at the same time and reduces the probability of merge. Thus, the heat flux is increased with the merge effect. In this case, the heat flux was increased by about 5% compared with the stochastic site distribution case under the 30K condition.

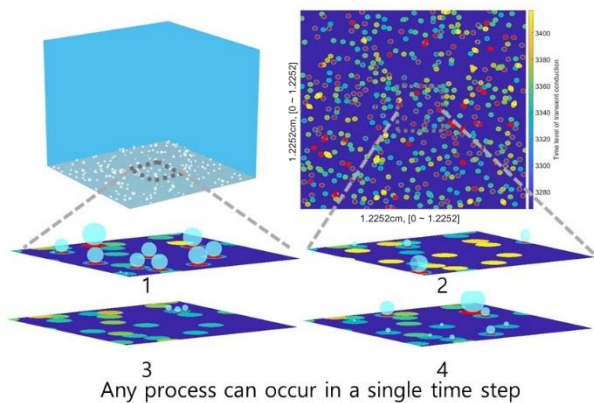


Fig. 9. Simulation results with stochastic nucleation timing

### 3. Conclusions

In this study, the boiling heat flux calculation was performed on an upward heating horizontal plate through the bubble tracking simulation. The RPI model was reproduced to validate the program and to investigate parametric effects of more realistic conditions. In this process, it was confirmed that the bubble merger has a significant effect on calculating the total heat flux. Therefore, applying additional models that can accurately predict the bubble merge effect would be necessary to accurately predict heat flux in an arithmetic way, such as the RPI model.

This model needs to be validated systematically again with boiling heat transfer experiments performed with high resolution measurement techniques such as Jung and Kim [9]. For further improvement of the numerical heat partitioning model described above, it requires to be parallelized to deal with a large number of bubbles and be coupled with CFD codes to replace the classical heat partitioning models.

### REFERENCES

- [1] N. Kurul and M. Z. Podowski, Multidimensional effects in forced convection subcooled boiling, *Int. Heat Transf. Conf.* 9, pp. 21–26, 1990.
- [2] N. Basu, G. R. Warrier, and V. K. Dhir, Wall heat flux partitioning during subcooled flow boiling: part 1—model development, *J. Heat Transfer*, vol. 127, no. 2, pp. 131–140, 2005.
- [3] J. Shi, R. Zhang, Z. Zhu, T. Ren, and C. Yan, A modified wall boiling model considering sliding bubbles based on the RPI wall boiling model, *Int. J. Heat Mass Transf.*, vol. 154, p. 119776, 2020.
- [4] L. Gilman and E. Baglietto, A self-consistent, physics-based boiling heat transfer modeling framework for use in computational fluid dynamics, *Int. J. Multiph. Flow*, vol. 95, pp. 35–53, 2017.
- [5] J. S. Kim and H. K. Cho, Advanced boiling heat transfer model for a horizontal tube with numerical analysis of bubble behaviours, *Int. J. Heat Mass Transf.*, vol. 175, p. 121168, 2021.
- [6] A. Khoshnevis, A. Sarchami, and N. Ashgriz, Effect of nucleation bubble departure diameter and frequency on modeling subcooled flow boiling in an annular flow, *Appl. Therm. Eng.*, vol. 135, pp. 280–288, 2018.

[7] R. Cole, A photographic study of pool boiling in the region of the critical heat flux, *AIChE J.*, vol. 6, no. 4, pp. 533–538, 1960.

[8] T. Hibiki and M. Ishii, Active nucleation site density in boiling systems, *Int. J. Heat Mass Transf.*, vol. 46, no. 14, pp. 2587–2601, 2003.

[9] S. Jung and H. Kim, Effects of surface orientation on nucleate boiling heat transfer in a pool of water under atmospheric pressure, *Nucl. Eng. Des.*, vol. 305, pp. 347–358, 2016.